Focusing on “the important” through targeted NMR experiments: An example of selective 13C-12C bond detection in complex mixtures

Faraday Discussions

Accepted Manuscript

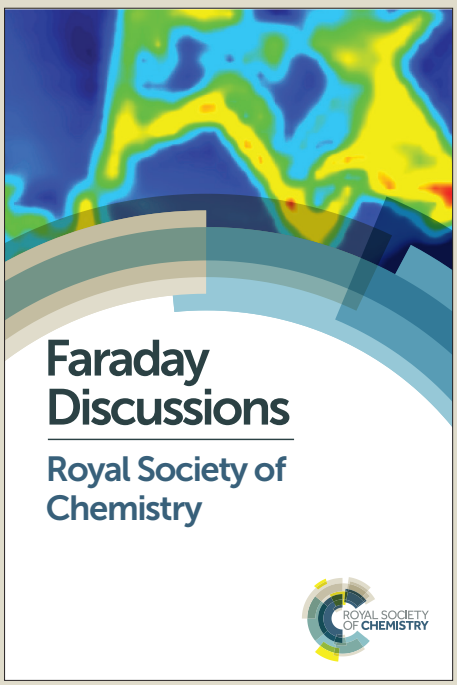

This article can be cited before page numbers have been issued, to do this please use: A. Jenne, R. Soong, W. Bermel, N. Sharma, A. Masi, M. Tabatabaei-Anraki and A. Simpson, *Faraday Discuss.*, 2018, DOI: 10.1039/C8FD00213D.

Journal Name

View Article Online
DOI: 10.1039/C8FD00213D

ARTICLE

Focusing on "the important" through targeted NMR experiments: An example of selective ^{13}C-^{12}C bond detection in complex mixtures

Received 00th January 20xx,
Accepted 00th January 20xx

DOI: 10.1039/x0xx00000x

www.rsc.org/

Amy Jenne,[a] Ronald Soong,[a] Wolfgang Bermel,[b] Nisha Sharma,[c] Antonio Masi,[c] Maryam Tabatabaei Anaraki,[a] and Andre Simpson[†a]

Current research is attempting to address more complex questions than ever before. As such, the need to follow complex processes in intact media and mixtures is becoming commonplace. Here a targeted NMR experiment is introduced which selectively detects the formation of ^{13}C-^{12}C bonds in mixtures. This study introduces the experiment on simple standards, and then demonstrates the potential on increasingly complex processes including: fermentation, *Arabidopsis thaliana* germination/early growth, and metabolism in *Daphnia magna* both *ex-vivo* and *in-vivo.* As signals from the intact ^{12}C and ^{13}C pools are themselves filtered out, correlations are only observed when a component from each pool combines (i.e. new ^{13}C-^{12}C bonds) in the formation of new structures. This targeted approach significantly reduces the complexity of the mixtures and provides information on the fate and reactivity of carbon in environmental and biological processes. The experiment has application to follow bond formation wherever two pools of carbon are brought together, be it the incorporation of ^{13}C enriched food into a living organism's biomass, or the degradation of ^{13}C enriched plant material in soil.

Introduction

Questions in science research are becoming increasingly complex, with biological and environmental relevance always at the forefront of discussion. Almost every natural sample including soils, atmospheric particles, plants, aquatic dissolved organic matter, and animals can be thought of as complex mixtures. Often isolation or fractionation can reduce complexity and make mixtures more amenable to a wider range of instrumental analyses. Conversely, it can be argued that it is often the synergism between components and phases in complex samples such as soil and living organisms that give rise to overall structure and function, and therefore must be kept intact.[1]

Nuclear Magnetic Resonance (NMR) spectroscopy is unique in that it is highly versatile and can be applied to liquids, gels, and solids. Thus it has applications to study both intact mixtures/systems or extracted/isolated sub-components.[2] NMR combines very high resolving capabilities, a diverse range of experiments to measure structure, dynamics, and interactions, while being non-invasive, and non-destructive.[3–6] The high resolving potential of NMR is often underestimated, but summarized beautifully by Hertkorn *et al.* The authors estimate 1D ^{1}H and ^{13}C NMR have peak capacities of ~3,000 and 30,000, while 2D ^{1}H-^{13}C increases to ~2,000,000 and 3D NMR to ~100,000,000.[7] On extrapolation to 7D NMR, which has recently been demonstrated on disordered proteins via sparse sampling approaches, the peak capacity can potentially reach on the order of 10^{18}.[8–10] Of course, in most environmental and biological samples, the limiting factor is a lack of sensitivity when dispersing signals into a larger number of higher dimensions. However, as NMR sensitivity continues to increase and sparse sampling approaches improve,[11] NMR experiments of high dimensionality become more feasible, and will therefore likely become central to the next generation of complex mixture research.[12] Arguably, one of the most impressive applications to date on environmental systems is by Bell *et al.*[13] Humic substances in soil have been described by many as the most complex known mixture.[14] Bell *et al.* combined selective labelling and 4D NMR to gain exquisite information on the lignin derived components from soil, with the approach identifying many of the exact structures for the first time.[13]

When performing mixture-based research there are two avenues that can be pursued, namely targeted and non-targeted analysis, for which NMR has strong capabilities in both. However, many analytical approaches are available for

[a] Environmental NMR Centre, University of Toronto, 1265 Military Trail, Toronto, ON, Canada, M1C 1A4.
[b] Bruker BioSpin GmbH, Silberstreifen 4 Rheinstetten, Germany.
[c] Department of Agronomy, Food, Natural Resources, Animals and the Environment, University of Padova, Padova, Italy.
† Corresponding author: andre.simpson@utoronto.ca

targeted analysis, while NMR's high reproducibility, non-destructive, and non-selective nature (i.e. any compounds containing an NMR active nucleus can be detected) make it uniquely suited for non-targeted analysis.[15] Deciding on a targeted or non-targeted approach is most commonly driven by the research question itself. For example, if the question is "what is the molecular composition of aquatic organic matter?", it would make sense that a researcher apply the highest resolution molecular tools available and try to evaluate what components make up the mixture as a whole in a non-targeted fashion.[16–18] Conversely, if the goal is to follow the fate of specific contaminants in soil, then having an NMR nucleus such as ^{19}F allows targeted monitoring of the contaminant and its interactions, providing information specific to the target of interest.[19] The study of Bell *et al.* was successful in identifying novel structural units because the ^{13}C enrichment targeted the lignin components in the soil organic matter.[13] In turn, this reduced the overlap with carbohydrates and allowed a wealth of new information to be uncovered. In both the targeted examples above, a specific NMR nucleus (^{13}C or ^{19}F) was introduced to provide the selectivity. In the current study, a slightly different approach is explored. Instead of monitoring a label selectively, the filtering is built into the NMR experiment itself. Here, a new experiment is developed that specifically targets the formation of ^{13}C-^{12}C bonds, where ^{13}C-^{13}C bonds and ^{12}C-^{12}C bonds are not detected by the experiment. This experiment could have widespread implications for any studies that bring two separate pools of carbon together and complements other experiments that are currently used for isotopic tracing by NMR.[20–22] For example, in 2006 a year-long study was performed following the fate of ^{13}C plant biomass as it degraded using HR-MAS NMR.[23] While humic substances are now thought to be largely complex mixtures,[24,25] at the time humic substances were thought to be chemically distinct, and formed from crosslinking components within soil organic matter.[26] As such, one of the goals of the 2006 study was to see if new bonds were formed. However, as the study followed just the fate of the ^{13}C enriched plant biomass, and as the material was so complex, while it was possible to see general changes (i.e. carbohydrates degraded fast, aliphatics accumulated etc.) it was not possible to definitely see if crosslinks formed between the ^{13}C enriched plant biomass and other components in the soil.[23] If this were to be repeated with the experiment introduced here, it should be possible to target only the new bonds between the ^{13}C-^{12}C which would help unravel how molecules are degraded, and if any novel recalcitrant structures do form within soil during humification. Additionally, the approach could have huge implications for monitoring and understanding the transfer of carbon in food webs. For example, *Daphnia magna* are a keystone aquatic species (a key food source for many fish) but cannot synthesize many lipids and sterols *de-novo,* and are reliant on algae for nutrition.[27] As such *D. magna* are one of the most studied species in ecology, yet details as to the individual molecular species, their sources, and their impact on growth is still not fully understood.[28] We anticipate that by utilizing targeted experiments that focus on ^{13}C-^{12}C bond formation, then detailed studies, that for example feed ^{13}C enriched *Daphnia* with ^{12}C algae (or vice versa), could provide insight on exactly how these organisms utilize food, and likely provide a better understanding of the biochemical pathways involved. Another example of a specific NMR experiment tailored for selective detection would be the amino acid-only experiment developed to selectively observe amino acid-profiles in living organisms.[29]

This study introduces the selective ^{13}C-^{12}C experiment, first on simple standards, and then demonstrates its potential on processes of increasing complexity including fermentation, plant growth, and *Daphnia* metabolism both *ex-vivo* and *in-vivo*. We anticipate that due to the versatility of NMR spectroscopy many more targeted experiments can be developed in the future that examine specific components or processes within complex environmental samples.

Experimental

Ethanol Fermentation

Ten milligrams of 1-^{13}C-Glucose (Sigma Aldrich) were dissolved into a 1.5 mL 90:10 water and D_2O solution. Baker's Yeast (Produced by ACH Food Companies Inc.) was added to the mixture, vortexed for 30 seconds, and then allowed to settle. The remaining suspension was then placed into a 5 mm NMR tube (Norell Inc. NJ, USA) and monitored inside the NMR instrument over 24 hours.

Daphnia magna Culturing

D. magna were cultured from a colony originally purchased from Ward's Scientific and maintained at 20°C, a water hardness of 124 mg $CaCO_3$ L^{-1}, and pH 7.5-8.5, consistent with local freshwater conditions. Cultures were kept under a 16:8 light/dark cycle. Species were fed 99% ^{13}C enriched *Chlamydomonas reinhardtii* (purchased from Silantes, GmbH)[30] as their sole food source for 14 days starting at birth, to produce enriched ^{13}C organisms. Daphnids were fed three times a week, and at the same time water was changed to ensure sufficient oxygen content. *D. magna* were also provided vitamin B_{12} (Sigma Aldrich, 2 µg/L) once a week to help with growth. Prior to NMR studies, organisms were placed in clean, aged water (dechlorinated via bubbling for one week) for 30 minutes to clear off residual algae. During the NMR experiments, the food source was switched to unenriched *Chlamydomonas reinhardtii* cultured in the lab using Bold's Basal Medium and following the Ministry of Ontario's Standard Operating Procedure for Algae Culturing.

Sterilization and Growth of *Arabidopsis thaliana*

The Wild-type Columbia (Col-0) *Arabidopsis thaliana* seeds (Originally from TAIR, OH, USA) were sterilized by a chlorine gas method. This method does not affect the seed viability, but removes microbial contaminants present on the seed surface.[31] The seeds in the Eppendorf tubes with the cap open were placed in the desiccator. 100 mL of bleach and 6 mL of

concentrated HCL (both from Sigma Aldrich) were placed inside the desiccator separately in a beaker. All the processes were performed inside the fume hood. After six hours of sterilization, the seeds were collected and stored in the freezer. The sterilized Wild-type Columbia (Col-0) *Arabidopsis thaliana* were grown in sterilized Murashige and Skoog (MS) growth medium containing 1% (w/v) glucose. For NMR experiments, uniformly labelled $^{13}C_6$-Glucose at 99% ^{13}C enrichment (Silantes, GmbH) was used. The seeds were then cold-stratified for three days. The plates with sterilized seeds were transferred to the dark for seven days at 21°C. Seedlings were collected on day zero, day one, day three, and day seven for NMR analysis.

Sample Preparation and Extraction of *D. magna and A. thaliana*

20 Fully labelled *D. magna* were removed from the culture, flash frozen with liquid nitrogen, and lyophilized. The remaining organisms were switched to natural abundance ^{13}C algae as their food source, and sampling was repeated every 24 hours for four days. Metabolites were extracted following the protocol by Nagato *et al.*[32] using 3.2 mg of dried sample in 65 µL of buffer and placed in 1.75 mm capillary tubes (Hirschmann, Eberstadt, Germany) for 2D NMR analysis.

A. thaliana samples were extracted using the protocol above prior to measurement, using 3.2 mg in 65 µL of buffer, and also in 1.75 mm tubes.

NMR Spectroscopy

NMR Experiments on Extractions

NMR experiments on extractions were performed using a Bruker Avance III 500 MHz NMR equipped with a ^{1}H-^{13}C-^{15}N TXI 1.7 mm microprobe fitted with an actively shielded gradient. The selective ^{13}C-^{12}C experiment is discussed in the main text. Data were collected with 98 increments, each with 16 scans (1-^{13}C-Glucose, 1,2-^{13}C-Glucose, and fermentation), and 64 increments with 832 scans (plants), and 896 scans (daphnids), 2048-time domain points, a recycle delay of one second, a 30ms or 80ms (see main text) TOCSY mixing time, a ^{1}J ^{1}H-^{13}C coupling of 145 Hz, and GARP-4 for decoupling. Presaturation (~100 Hz bandwidth) was applied during the recycle delay to help reduce large water signals when required. The 90° pulses were determined in each sample. Data were processed with a sine-squared function phase shifted by 90° in both dimensions and a zero-filling factor of 2.

In-vivo Flow System

A low-volume flow system was utilized for these experiments. This was accomplished using the system and method created by Tabatabaei Anaraki *et al*.[33] 40 *Daphnia* all 14 days old (fed only ^{13}C algae from birth), were placed in a high-precision, thin-walled 5 mm NMR tube (Wilmad-LabGlass, NJ, USA), with a Teflon plug (machined in-house) placed in the bottom of the NMR tube to prevent the daphnids from swimming outside the coil region. The top plug was created out of Teflon to keep the injection capillary glass and D_2O capillary in place (created in-house), and to keep all the daphnids within the coil region, maximizing signal. The flow rate was set at 0.25 mL/min, and the reservoir contained oxygenated water and unenriched algae. This enables the daphnids to survive, and remain in a low-stress environment in the instrument by providing consistent food and oxygen. The entire system is placed inside the NMR and kept at 5°C to slow down the movement of the daphnids, enabling better water suppression and more stable signal. Separate *in-vivo* NMR experiments were conducted for 24 hours on fully enriched ^{13}C D*aphnia*, and *Daphnia* after being fed ^{12}C algae outside of the instrument for nine days.

In-vivo NMR Experiments

Experiments were performed on a Bruker Avance III HD 500 MHz (^{1}H) NMR spectrometer using a ^{1}H-^{13}C-^{15}N TCI Prodigy cryoprobe fitted with an actively shielded z-gradient. The external D_2O capillary lock (~5 µL) was integrated into the flow system and all experiments were run locked. The ^{13}C-^{12}C experiment was performed as with extracts, with the exception that the reversed editing block was removed to increase SNR and reduce relaxation. Presaturation (~100 Hz bandwidth) was applied during the recycle delay to help reduce the large water signal. 90° pulses determined in each sample and a TOCSY mixing time of 30ms was used. A total of 128 increments were collected, each with 480 scans, 2048-time domain points, and a recycle delay of one second. The INEPT transfer was based on ^{1}J ^{1}H-^{13}C coupling of 145 Hz. Data were processed with a sine-squared function phase shifted by 90° in both dimensions and a zero-filling factor of 2.

Spectral Assignments

Compound identification and assignment were done using AMIX (Analysis of MIXtures software package, version 3.9.15, Bruker BioSpin, in combination with the Bruker Bio-reference NMR databases version 2-0-0 through 2-0-5. Spectra were calibrated against the Bruker Bio-reference NMR databases using Tyrosine and D-glucose resonances for reference. Assignment was performed using a procedure previously described.[34,35]

Results and Discussion

Basic Pulse Sequences and Spectra

Figure 1 shows the basic sequence used for the selective detection of ^{13}C-^{12}C bonds. In practice, sequences A and B are acquired in an interleaved fashion such that slice one of the 2D is the result from sequence A, and slice two is the result of sequence B. The datasets are split after acquisition to yield separate datasets. As A is essentially a "reference" for B it is important to collect the data sets at similar time points which is the purpose of interleaving the acquisition.

The result of sequence A is a standard reverse HSQC where the CH_2 moieties are reflected around the carbon offset (O_2P).[36] The advantage is that in complex samples the editing

improves spectral dispersion and helps reduce overlap especially in the aliphatic region where chemical shift overlap between $CH/CH_2/CH_3$ is common. The added dispersion will become clearer in more complex samples shown later in the manuscript (see Figure 4 as an example).

Figure 1 inset 1 shows the results from sequence A on glucose labelled with ^{13}C at the 1-position (1-^{13}C-Glucose). As position one is a C-H group, the result from sequence A in this case is the same as a conventional HSQC spectrum and two cross peaks arise, one from α-glucose and one from β-glucose. In Figure 1-2 the adiabatic TOCSY block is activated, and protons attached to ^{13}C are now allowed to mix with all other protons in the sample (both those attached to ^{13}C and those attached to ^{12}C). The result is similar to an HSQC-TOCSY experiment, with relays along the horizontal plane. Readers should note that the dataset in Figure 1-2 is not actually recorded using sequence B, but is included as an additional step to make it easier to visualize how the experiments work (i.e. progressing from Figure 1-1 through 1-3). An adiabatic TOCSY[37] is used as it shows superior mixing in complex natural samples over MLEV and DIPSI.[3,38]

The result of the full sequence B is shown in Figure 1-3. After the TOCSY block and additional ^{13}C filter is applied between 1-2 and 1-3, the signals from any protons attached to ^{13}C are cancelled. The final result is the ^{1}H attached to ^{12}C are selectively detected. It is important to note that for peaks to occur in the first place they must be in the same ^{1}H-^{1}H spin system as a ^{13}C nucleus. If a molecule contained only ^{1}H-^{12}C then the protons would not be selected by the first block. If a molecule contains all ^{13}C then the last filter would cancel the signals such that they are not detected. As such the experiment selectively detects ^{13}C-^{12}C in proximity (albeit via their attached protons as ^{12}C is NMR inactive). The maximum number of bonds between the ^{13}C and ^{12}C that can be detected is determined by the TOCSY mixing time. In this first example 80ms is used, as such, correlations from the ^{13}C labelled 1-position relay around most of the glucose ring and a number of short (COSY), and long (TOCSY) correlations are seen. However, if the TOCSY mixing time is reduced to 30ms mainly COSY type interactions are emphasized. In complex samples this can reduce crowding in data and make it a little easier to interpret. Conversely, additional long range TOCSY correlations can be useful in aiding spectral assignment.

Figure 2 shows the results of sequence B performed on 1-^{13}C-Glucose using a 30ms mixing time for comparison to Figure 1, such that only the COSY correlations to ^{12}C show. The result being that only the ^{12}C directly adjacent to ^{13}C are selected. When the result of sequence A (Figure 2A) and sequence B (Figure 2B) are overlaid (Figure 2C) the one bond ^{1}H-^{13}C crosspeaks are blue while correlations to the ^{12}C adjacent are shown in red. We find this differential colouring approach very convenient for visualizing datasets, if a red and blue crosspeak appear on the same horizontal row, this indicates a ^{13}C and ^{12}C unit are directly bonded. Interpretation from assigned NMR databases is easy, as HSQC crosspeaks are commonly labelled with the corresponding structural position (H1/C1, H2/C2 etc.). In the example shown in Figure 2, first the blue cross peaks (one bond correlations of ^{1}H-^{13}C) are identified and then using the assigned molecular structure, the crosspeak (and thus chemical shifts) of the adjacent ^{1}H-^{12}C unit are found. If the molecule selected for assignment is indeed correct, then the proton chemical shift of the relay should match the proton chemical shift at the same position in the molecule of interest. In the case of 1-^{13}C-Glucose, the relays match exactly with the proton chemical shifts of carbon 2 in both α-glucose and β-glucose as expected. If assigned molecules are not available in a database, then assignments could be performed by referring to the HSQC and COSY (or TOCSY when a longer mixing time is used) data in combination. The one bond correlation would be identified from the HSQC data and the chemical shift of the proton relay from the COSY data. Whichever way the assignment is performed the experiment gives a convenient approach to monitor the formation of ^{13}C-^{12}C bonds.

A Simple Process: Fermentation

To demonstrate the concept further, 1-^{13}C-Glucose was allowed to ferment in the presence of Baker's yeast (*Saccharomyces cerevisiae)* to form ethanol over 24 hours inside the NMR. Figure 3A shows the overlaid one-bond/relay data before the experiment began, which is essentially identical to that shown in Figure 2C. After 24 hours of fermentation, ethanol has formed. In Figure 3B, it can be seen that the CH_3 group in the ethanol has been derived from the ^{13}C labelled 1-position (blue contour) while the CH_2 group is from ^{12}C (red contour). This is consistent with the well understood process of fermentation of glucose. Under anaerobic conditions, glucose breaks down to form ethanol, with the help of ATP and NADP/H. Through this process the six-membered ring breaks, resulting in two 3-carbon pyruvate derivatives, which are then broken down into 2-ethanol. Through this process, the result is a ^{13}C in the 1 position, and a ^{12}C in the 2 position.[39,40] A simplified mechanism of the fermentation process can be seen in Figure 3C.

A Complex Process: *Daphnia Magna Ex-Vivo*

Figure 4 demonstrates the approach in a much more complex system. In this case *Daphnia magna* have been fed 99% ^{13}C enriched algae two weeks from birth such that the overwhelming majority of carbon in their biomass is ^{13}C. After this they were fed ^{12}C algae (natural abundance ^{13}C) for 96 hrs. During this time, it is expected that ^{13}C-^{12}C bonds will form as their new ^{12}C food is incorporated into their ^{13}C biomass. A TOCSY time of 80ms is used in this example such that both long- and short-range correlations are observed. Samples were taken every 24 hours over four days and extracted using a phosphate buffer. Figure 4A shows the result after 96 hours. The CH_2 in the reversed HSQC are flipped around the carbon offset (100 ppm in this case) and appear in the lower right quadrant of the data set. CH_3 and CH appear as they would in a conventional HSQC experiment. The data are highly complex, and the full analysis is beyond the scope of this paper. However, five regions of interest have been highlighted.

Region one is consistent with a relay from the adenine group to the ribose ring in energy molecules (i.e. ATP, ADP, and AMP). This indicates the adenine is coming from the older ^{13}C carbon pool while the ribose has been synthesized from the ^{12}C biomass introduced over the last 96 hours.[41,42] In this case, the adenine and ribose link via a quaternary N center and protons on each side of this (one from adenine and one from ribose) TOCSY correlate due to the 80ms mixing. This has been confirmed by cross-checking the TOCSY spectra of energy molecules (ATP, ADP, AMP) in Bruker bio-reference databases which all show this correlation.[35] The formation of energy molecules from carbon coming from different pools is consistent with the glycolysis and glycogenesis pathways used by *D. magna* for energy formation. These are major energy-creating pathways in crustaceans producing vital ATP and NAD/H.[43] Pyruvate is formed from the breakdown of the glucose contained within the algae, and given the cyclic nature of the tricarboxylic acid (TCA) cycle, these pyruvate molecules can come from either labelled or non-labelled algae. These pyruvate molecules then form into new energy containing molecules that are used by *D. magna*. This process has been studied extensively using cell flux analysis with *E. coli* and *S. cerevisiae.* Upon adding labelled glucose into the system, energy metabolism can be monitored and is seen to occur via the glycolysis/glycogenesis pathway.[42,44–46] By our estimate, this may be the first time this process has been examined directly in *D. magna.*

Region two is consistent with relays from ^{13}C enriched lipids to ^{12}C lipids containing double bonds. *Daphnia* are known to assimilate most of their lipids from their diet and cannot synthesize many essential fatty acids from scratch.[27,47–49] As the food source is changed to unenriched algae, the D*aphnia* begin to form lipids from the new food source. Acetyl CoA, derived from pyruvate and the degradation of glucose, is used as a primer for the carbon chain, and elongated by the repeating condensation of malonyl-CoA yielding lipid pools.[50,51] As well, some dietary fatty acids are able to be desaturated in the carboxyl direction, as opposed to the methyl direction and then elongated to form polyunsaturated fatty acids.[50] The correlation between ^{13}C-^{12}C in the lipid chains suggest existing lipids are being modified with units derived from the new ^{12}C food source.

Region three is consistent with protons in ^{13}C lipid chains relaying to the ^{12}C adjacent to an oxygen such as in a phospholipid head or even an ester group. This follows the above explanation where the formation of phospholipids to lipids occurs through dietary routing, which is the process of linking together multiple fatty acid or lipid chains through digestion, where the chains can be from different carbon pools.[50]

Region four are carbohydrates including glucose breakdown and formation. As the experiment uses an 80ms TOCSY spinlock, coupling around the entire hexose ring is expected. As such the correlations indicate that ^{12}C and ^{13}C are being brought together to form the carbohydrates. This is consistent with the process explained above in the breakdown of glucose through glycolysis and then the re-formation through glycogenesis. As there will be pools of ^{13}C pyruvate and ^{12}C pyruvate the glucose can get re-formed with ^{12}C theoretically in any position, resulting in ^{13}C-^{12}C relays observed within glucose.[52]

Region five is consistent with α-protons in amino acids relaying to the side chains. The peaks are the closest match for a mixture of glutamine and glutamate. This is consistent with studies in rat brains which quickly assimilate glucose into glutamate.[46,53] After this, glutamine can be formed from the glutamate by glutamine synthetase.[54,55] The fact that ^{13}C and ^{12}C are found in the same system suggest that both ^{12}C and ^{13}C are feeding the glutamate-glutamine cycle which produces amino acids containing both isotopes.[56] Glutamine and glutamate are used by *Daphnia magna* to aid in glucose metabolism similar to a wide range of species.[56]

While the 2D NMR data contains a wealth of information down to the exact bonds involved in key processes, the ^{1}H projections represent a complementary source of information. As explained above the only ^{1}H signal remaining at the end of pulse sequence B are relays to ^{1}H-^{12}C that are in close proximity to ^{13}C. As such the ^{1}H projection essentially gives a simple visual as to the fate of ^{12}C as a process progresses. Consider, for example, the ^{13}C *Daphnia* feeding on ^{12}C algae. At the start of the experiment, the *Daphnia* are fully ^{13}C enriched so no signal is expected in the ^{13}C-^{12}C experiment or its ^{1}H projection. However, overtime as the *Daphnia* utilize the ^{12}C, new molecules are formed bringing together both ^{13}C and ^{12}C, and signal will appear in the ^{13}C-^{12}C experiment. In turn, the ^{1}H projection shows the fate of the ^{12}C and what type of molecules it has become incorporated into. Figure 4B shows the ^{1}H projections over time as the *Daphnia* utilize ^{12}C. At time zero the spectrum is essentially blank, as expected. However, some small signals are present consistent with an adenine group. Prior to lyophilizing, the *Daphnia* were transferred and stored in aged water (which itself contains an algal background) for ~30 min. It is likely the *Daphnia* used this ^{12}C to start making adenine, the precursor required for energy molecules such as ADP/ATP/AMP.

After 24 hours of exposure to the unenriched food ^{12}C has been incorporated into a range of structural categories. Signals from energy molecules have become much stronger, and key ribose signals around 6 ppm start to appear indicating a portion of both the adenine and ribose units are being made from ^{12}C substrates and are being brought in proximity to ^{13}C. In addition, a range of amino acids and carbohydrate signals also appear. It is important to remember that to appear in the spectrum a ^{13}C and ^{12}C must be bonded together somewhere in the molecule, as such the experiment selectively detects new molecules that had to have been synthesized *de-novo* from the food source. After 55 hours the spectral profile is relatively similar with the exception of carbohydrates that have ~doubled in intensity, consistent with the newly introduced ^{12}C biomass being combined with ^{13}C likely for energy via glycolysis.[42,46] After 96 hours a distinct broad signal is noted around 1.2 ppm consistent with $(CH_2)_n$ in lipids. This indicates the *Daphnia* are modifying ^{13}C lipids using ^{12}C from their food source. This is particularly interesting, as mentioned

above *Daphnia* cannot synthesize many lipids and rely on their food to assimilate many essential fatty acids. In addition, the lipids incorporated from their diets are key for reproduction. As *Daphnia* reproduce asexually, the lipid content is required for egg formation, and spikes immediately prior to birth, which is on average every 2-3 days.[57] Daphnids without proper lipid content stop producing viable offspring, and will often start to convert to sexual reproduction.[58] Thus, the use of lipids in *Daphnia* is key to their survival. Further, as *Daphnia* are keystone species, the stable reproductive cycles are imperative for many species' survival. *Daphnia* are found in almost every fresh water body worldwide, and are the food source for many other aquatic species.[48,59,60] Therefore, the use of lipids is not only key to *Daphnia* survival, but also has many potential negative consequences to higher trophic levels (i.e. fish and higher predators) based on available food sources. As such the ^{13}C-^{12}C experiment introduced here specifically targets the modification of existing ^{13}C lipids by ^{12}C, and could be quite important in uncovering a better understanding of lipid modification and utilization in key species such as *Daphnia*.

Working in Reverse: $^{13}C_6$-Glucose in *Arabidopsis thaliana*

Figure 5 depicts the germination and early growth of ^{12}C *Arabidopsis thaliana* seeds in the dark using $^{13}C_6$-Glucose as the sole carbon source as previously described.[61] This study has been designed as the reverse of the *Daphnia* study such that the process begins with ^{12}C carbon, and ^{13}C is added into the system. As the plants are stored in the dark, photosynthesis does not occur, and the seeds grow via ^{13}C sorption through its husk and later uptake via roots after initial germination. In this situation, the question becomes "what does the plant synthesize from the ^{12}C stored in its seeds?" As original biomass in the seeds is the only source of ^{12}C, the only way structures can appear is if the carbon from seed biomass is combined with ^{13}C derived from the glucose, forming a new structure. After one day of germination/growth, no new signals are seen (see small inset in Figure 5A). However, after one week of growth, the plant extract shows three main types of signals arising from several different pathways. There are three sections that are worth highlighting in Figure 5B.

In region one, the new peaks arise from the synthesis of glutamate. This amino acid is crucial in the health of plants as it is used for assimilation and dissimilation of ammonia that is then transferred to all other amino acids in the plant.[62] As well, glutamate has been shown to be the precursor to chlorophyll synthesis in developing leaves.[62] Glutamate, like many of the metabolites under examination, is formed through the TCA cycle in plants and animals, therefore it also has implications in regards to energy formation.[56,63] Given the importance of this amino acid to plant health, it is expected that its formation would occur relatively quickly in the growth of *Arabidopsis.* In this experiment $\alpha^{13}C$-$\beta^{12}C$ (peak 1A) and $\alpha^{12}C$-$\beta^{13}C$ relays (peak 1B) are seen for glutamate indicating ^{12}C and ^{13}C pools are likely brought together from isotopically different sources via the TCA cycle.

Region two represents relays from the ^{13}C portions of glucose to ^{12}C at the 1-position. As a TOCSY mixing time of 80ms was used for the plant study, long range interactions around the ring will be observed. Plants, like all living things, use glucose as an energy source for ATP formation, and without light, the glycolysis process occurs much like in *Daphnia.* The glucose gets broken down into two pyruvate molecules, and then moves through the TCA cycle to form ATP.[64,65] However, pyruvate can also move 'backwards' through gluconeogenesis to reform glucose, but the two pyruvates can be from different carbon sources. This results in a glucose molecule with C1-3 with one isotope and C4-6 as another.

Region three represents energy molecules such as ATP/ADP/AMP with a ^{13}C adenine connecting to a ^{12}C ribose ring. Much like in the *Daphnia*, the plants utilize the glucose through the TCA cycle to create energy molecules.[44,45] The results here indicate that a portion of the energy molecules are created when adenine derived from the $^{13}C_6$-glucose is combined with ribose derived from the seed (^{12}C).

Daphnia magna In-vivo

To further test the applicability of the ^{13}C-^{12}C experiment, the sequence was applied to a flow system containing living *Daphnia* raised on ^{13}C from birth. The main difference here is that the editing step has been removed from the sequence in Figure 1B such that the CH_2 groups are not flipped around the ^{13}C offset. The reason for this is that in intact samples such as living *Daphnia*, relaxation is very fast. Therefore, it is prudent to reduce the pulse sequence length as much as possible. When the CH_2 edited step was removed, it was found the signal intensity doubled over the edited version *in-vivo*. Due to the additional signal, the non-edited version was applied to the *in-vivo* system.

Figure 6A shows a conventional HSQC experiment for reference, which represents all the ^{1}H-^{13}C bonds in the sample. Figure 6B shows the result of the ^{13}C-^{12}C experiment of the *Daphnia* grown solely with ^{13}C algae since birth. As the organisms contain only ^{13}C, no signals appear in the ^{13}C-^{12}C experiment. Note, the vertical streak centered around 5 ppm is the breakthrough of residual water due to the fact that the organisms are swimming in 100% pure H_2O and 90% of their bodies are also water, making perfect water suppression incredibly difficult. Figure 6C shows the same culture of organisms after nine days of being fed ^{12}C carbon. As can be seen, ^{12}C has been incorporated into the original ^{13}C biomass at various sites. Interestingly, despite the complexity of the system, all the correlations are relatively easy to assign based on the literature,[66–68] and arise from the modification of lipids (see Figure 6D). Various structures can be identified, most of which appear twice with the relative locations of the ^{13}C and ^{12}C switched. This suggests that the *Daphnia* can utilize the ^{12}C and ^{13}C pools in similar ways. For example, it indicates the organisms can modify ^{13}C lipids from their own biomass with ^{12}C from their new diet. It also suggests they can modify ^{13}C

lipids from their new diet using ^{12}C carbon derived from their own biomass.

As discussed previously, *Daphnia* are limited in the lipids they can make, thus lipid incorporation from their diet is very important.[48,57,58] The expectation is that modification of their food source, and lipids from their own biomass will result in new peaks formed using this sequence. For example, as the organism digests the algae, the lipids are broken down into single chain fatty acids that can then be desaturated and elongated using carbon already in the system.[50] Such lipids can be utilized to make more complex chains of lipids with additional carbon coming from either the diet (^{12}C) or biomass (^{13}C) pools.[69,70] This would occur relatively quickly and in higher concentrations compared to other metabolites due to the energy requirement from the lipids, and the inability to synthesize them internally. This experiment is a powerful approach to providing information in a complex *in-vivo* system for processes such as lipid modification that are currently not well understood.[28]

The Future Potential for Quantification

The ability to quantify the ratio of $^{12}C/^{13}C$ at a given position in a molecule would be extremely useful in constrained metabolic models, and tracing pathways.[71,72] Using the sequence outlined in Figure 1B it is not possible to quantify the $^{12}C/^{13}C$ ratio as the intensity of the cross peaks depends on both the efficiency of the TOCSY transfer and the abundance of ^{12}C in the peaks. Unfortunately, a rigorous implementation of a quantitative approach is beyond the scope of this paper and would likely take years of research to implement thoroughly in complex systems. That said, it is worthwhile to consider the future potential for quantification on a standard that paves the way for development and further discussion.

Figure 7 shows two pulse sequences that when used in combination, in theory, should permit quantification of site specific $^{13}C/^{12}C$ ratios. The result of Figure 7B is in fact identical to Figure 1B (i.e. relays to ^{12}C remain, while ^{13}C is subtracted). Figure 7A is derived from 7B with the goal to keep the pulses, durations, and timing identical between the two sequences. After the TOCSY proton magnetisation is excited and the CH coupling evolves for 1/2J, either block A or B are executed. In case of B, the first ^{13}C 90° pulse converts the magnetisation into unobservable zero and double quantum coherence. Remaining proton magnetisation can again evolve into CH antiphase magnetisation which then is also converted into unobservable magnetisation by a second ^{13}C 90° pulse, thus enhancing the efficiency of the filter. For block A the position of the second 90° pulse (of B) is changed (moved to the beginning). These two ^{13}C 90° pulses now act as a 180° pulse and reverse the J evolution so that at the end of block A all the magnetisation is back in phase and no filtering takes place. The net result is that sequence 7A now allows both protons attached to both ^{1}H-^{13}C, and ^{1}H-^{12}C signals pass, while sequence 7B blocks the ^{1}H-^{13}C signals. As the timing in both sequences is identical, Figure 7A acts as a reference for the sequence shown in Figure 7B. As such we will refer to the sequence in Figure 7A as the "quantitative reference" while we will refer to the sequence in 7B as the "^{12}C-only sequence." The TOCSY transfer in both will be identical, as such, the difference in signal intensity between the reference and the ^{12}C-only sequence will be from the subtraction of the ^{13}C signal. The concept is best explained on a standard. Figure 7 panel 1 shows the result from 99% 1,2-^{13}C-Glucose. Two horizontal bands appear, the upper band representing correlations between the 2-^{13}C position and protons around the ring, with the lower band representing correlations between the 1-^{13}C position and the ring protons. As there is no X filter, both protons attached to ^{12}C and ^{13}C appear in the spectrum. Figure 8A (top spectrum) shows the proton projection from the experiment. Conversely, Figure 7 panel 2 shows the result with the X filter turned on such that the ^{13}C signals subtract. The corresponding projection is shown in Figure 8A (bottom spectrum). Figure 8B shows the spectra superimposed and it is clear the intensity from protons on ^{12}C are near identical in both experiments while those from ^{13}C are completely suppressed. As such the ratio between the two spectra indicates the ^{13}C positions are essentially fully labelled (99%) while the ^{12}C positions are essentially ^{13}C free. In reality, of course, the ^{12}C position will be at natural abundance and should contain ~1.1% ^{13}C. Looking at the peaks, there is a very slight reduction that is consistent with a 1% reduction in signal at the "^{12}C-position," but the accuracy and reproducibility of this would need to be the subject of a much more extensive study. Future work would need to focus on standards with different levels of ^{13}C enrichment to assess how well ratios can be determined and the errors associated with such measurements, before measurements in complex systems would be meaningful. The goal here is simply to introduce one possible route towards isotope ratio quantification in products that are formed when ^{12}C and ^{13}C are bonded together in a complex process, that is a natural extension of the qualitative experiments introduced in the main body of this work.

Conclusions

A new method of examining new bond formation using targeted 2D NMR has been explored. With this new sequence ^{13}C-^{12}C bond formation can be selectively observed. To show the concept, processes from simple fermentation to complex metabolic examination in *Daphnia magna* and *Arabidopsis thaliana* were examined both *ex-vivo* and *in-vivo*. The results provide insight into how these species utilize food and energy sources and synthesize new molecules such as glutamate, ATP, and lipids. Quantification is briefly considered, and the sequence is modified to provide site specific $^{13}C/^{12}C$ ratios within a simple standard. However, additional further characterization with partially labelled standards is required to determine the error of such measurements before application to complex systems.

In summary, the approach provides a unique insight into the fate and reactivity of carbon in environmental and biological samples. After detailed spectral interpretation, it

should be a useful tool in understanding how organisms utilize, store, and transform carbon. Similarly, in environmental research, the transformation and fate of organic matter are of widespread interest. If an enriched substrate (for example, ^{13}C enriched plant biomass, ^{13}C enriched biochar, or a ^{13}C enriched contaminant) is introduced in soil, sediment or water, the experiment should identify when these materials become functionalized, or degraded and recombined with ^{12}C from their environment. In turn, this should provide better insight into carbon sequestration, carbon cycling, humification, and contaminant fate.

Conflicts of interest

There are no conflicts to declare.

Acknowledgements

Andre Simpson would like to thank the Strategic (STPGP 494273-16) and Discovery Programs (RGPIN-2014-05423), the Canada Foundation for Innovation (CFI), the Ontario Ministry of Research and Innovation (MRI), the Krembil Foundation for providing funding, and the Government of Ontario for an Early Researcher Award.

Notes and references

1 A. J. Simpson, Y. Liaghati, B. Fortier-McGill, R. Soong and M. Akhter, Perspective: in vivo NMR - a potentially powerful tool for environmental research, *Magn. Reson. Chem.*, 2015, **53**, 686–690.

2 D. Courtier-Murias, H. Farooq, H. Masoom, A. Botana, R. Soong, J. G. Longstaffe, M. J. Simpson, W. E. Maas, M. Fey, B. Andrew, J. Struppe, H. Hutchins, S. Krishnamurthy, R. Kumar, M. Monette, H. J. Stronks, A. Hume and A. J. Simpson, Comprehensive multiphase NMR spectroscopy: Basic experimental approaches to differentiate phases in heterogeneous samples, *J. Magn. Reson.*, 2012, **217**, 61–76.

3 A. J. Simpson, D. J. McNally and M. J. Simpson, NMR spectroscopy in environmental research: From molecular interactions to global processes, *Prog. Nucl. Magn. Reson. Spectrosc.*, 2011, **58**, 97–175.

4 P. R. L. Markwick, T. Malliavin and M. Nilges, Structural Biology by NMR: Structure, Dynamics, and Interactions, *PLoS Comput. Biol.*, 2008, **4**, e1000168.

5 R. Ghose, in *eLS*, John Wiley & Sons, Ltd, Chichester, UK, 2017, pp. 1–20.

6 M. Nilsson, Diffusion NMR, *Magn. Reson. Chem.*, 2017, **55**, 385–385.

7 N. Hertkorn, C. Ruecker, M. Meringer, R. Gugisch, M. Frommberger, E. M. Perdue, M. Witt and P. Schmitt-Kopplin, High-precision frequency measurements: indispensable tools at the core of the molecular-level analysis of complex systems, *Anal. Bioanal. Chem.*, 2007, **389**, 1311–1327.

8 S. Żerko and W. Koźmiński, Six- and seven-dimensional experiments by combination of sparse random sampling and projection spectroscopy dedicated for backbone resonance assignment of intrinsically disordered proteins, *J. Biomol. NMR*, 2015, **63**, 283–90.

9 X. Yao, S. Becker and M. Zweckstetter, A six-dimensional alpha proton detection-based APSY experiment for backbone assignment of intrinsically disordered proteins, *J. Biomol. NMR*, 2014, **60**, 231–240.

10 S. Hiller, C. Wasmer, G. Wider and K. Wüthrich, Sequence-Specific Resonance Assignment of Soluble Nonglobular Proteins by 7D APSY-NMR Spectroscopy, *J. A. Chem. Soc.*, 2007, **129**, 10823–10828.

11 M. Mobli, M. W. Maciejewski, A. D. Schuyler, A. S. Stern and J. C. Hoch, Sparse sampling methods in multidimensional NMR, *Phys. Chem. Chem. Phys.*, 2012, **14**, 10835–43.

12 C. Pontoizeau, T. Herrmann, P. Toulhoat, B. Elena-Herrmann and L. Emsley, Targeted projection NMR spectroscopy for unambiguous metabolic profiling of complex mixtures, *Magn. Reson. Chem.*, 2010, **48**, 727–733.

13 N. G. A. Bell, A. A. L. Michalchuk, J. W. T. Blackburn, M. C. Graham and D. Uhrín, Isotope-Filtered 4D NMR Spectroscopy for Structure Determination of Humic Substances, *Angew. Chem. Int. Ed. Engl.*, 2015, **54**, 8382–5.

14 I. M. Young and J. W. Crawford, Interactions and self-organization in the soil-microbe complex, *Science*, 2004, **304**, 1634–7.

15 J. L. Markley, R. Brüschweiler, A. S. Edison, H. R. Eghbalnia, R. Powers, D. Raftery and D. S. Wishart, The future of NMR-based metabolomics, *Curr. Opin. Biotechnol.*, 2017, **43**, 34–40.

16 N. Hertkorn, M. Frommberger, M. Witt, B. P. Koch, P. Schmitt-Kopplin and E. M. Perdue, Natural Organic Matter and the Event Horizon of Mass Spectrometry, *Anal. Chem.*, 2008, **80**, 8908–8919.

17 B. P. Koch, M. Witt, R. Engbrodt, T. Dittmar and G. Kattner, Molecular formulae of marine and terrigenous dissolved organic matter detected by electrospray ionization Fourier transform ion cyclotron resonance mass spectrometry, *Geochim. Cosmochim. Acta*, 2005, **69**, 3299–3308.

18 N. Hertkorn, M. Harir, B. P. Koch, B. Michalke and P. Schmitt-Kopplin, High-field NMR spectroscopy and FTICR mass spectrometry: powerful discovery tools for the molecular level characterization of marine dissolved organic matter, *Biogeosciences*, 2013, **10**, 1583–1624.

19 H. Masoom, D. Courtier-Murias, R. Soong, W. E. Maas, M. Fey, R. Kumar, M. Monette, H. J. Stronks, M. J. Simpson and A. Simpson, From Spill to Sequestration: The Molecular Journey of Contamination via Comprehensive Multiphase NMR, *Environ. Sci. Technol.*, 2015, **49**, 13983–13991.

20 I. A. Lewis, R. H. Karsten, M. E. Norton, M. Tonelli, W. M. Westler and J. L. Markley, NMR Method for Measuring Carbon-13 Isotopic Enrichment of Metabolites in Complex Solutions, *Anal. Chem.*, 2010, **82**, 4558–4563.

21 P. N. Reardon, C. L. Marean-Reardon, M. A. Bukovec, B. E. Coggins and N. G. Isern, 3D TOCSY-HSQC NMR for Metabolic Flux Analysis Using Non-Uniform Sampling, *Anal. Chem.*, 2016, **88**, 2825–2831.

22 T. W. M. Fan and A. N. Lane, NMR-based stable isotope resolved metabolomics in systems biochemistry, *J. Biomol. NMR*, 2011, **49**, 267–80.

23 B. P. Kelleher, M. J. Simpson and A. J. Simpson, Assessing the fate and transformation of plant residues in the terrestrial environment using HR-MAS NMR spectroscopy, *Geochim. Cosmochim. Acta*, 2006, **70**, 4080–4094.

24 B. P. Kelleher and A. J. Simpson, Humic Substances in Soils: Are They Really Chemically Distinct?, *Environ. Sci. Technol.*, 2006, **40**, 4605–4611.

25 M. W. I. Schmidt, M. S. Torn, S. Abiven, T. Dittmar, G. Guggenberger, I. A. Janssens, M. Kleber, I. Kögel-Knabner, J. Lehmann, D. A. C. Manning, P. Nannipieri, D. P. Rasse, S. Weiner and S. E. Trumbore, Persistence of soil organic matter as an ecosystem property, *Nature*, 2011, **478**, 49–56.

26 M. H. B. Hayes, *Humic substances II: in search of structure*, J. Wiley, 1st edn., 1989.

27 N. Sengupta, D. C. Reardon, P. D. Gerard and W. S. Baldwin, Exchange of polar lipids from adults to neonates in Daphnia magna: Perturbations in sphingomyelin allocation by dietary lipids and environmental toxicants, *PLoS One*, 2017, **12**, 1–25.

28 D. Martin-Creuzburg, E. von Elert and K. H. Hoffmann, Nutritional constraints at the cyanobacteria- *Daphnia magna* interface: The role of sterols, *Limnol. Oceanogr.*, 2008, **53**, 456–468.

29 D. Lane, R. Soong, W. Bermel, W. Maas, S. Schmidt, H. Heumann and A. Simpson, in *57th Experimental NMR Conference*, Pittsburg, 2016.

30 R. Soong, E. Nagato, A. Sutrisno, B. Fortier-Mcgill, M. Akhter, S. Schmidt, H. Heumann and A. J. Simpson, In vivo NMR spectroscopy : toward real time monitoring of environmental stress, *Magn. Reson. Chem.*, 2015, 774–779.

31 B. E. Lindsey, L. Rivero, C. S. Calhoun, E. Grotewold and J. Brkljacic, Standardized Method for High-throughput Sterilization of Arabidopsis Seeds, *J. Vis. Exp.*

32 E. G. Nagato, B. P. Lankadurai, R. Soong, A. J. Simpson and M. J. Simpson, Development of an NMR microprobe procedure for high-throughput environmental metabolomics of Daphnia magna, *Magn. Reson. Chem.*, 2015, **53**, 745–753.

33 M. Tabatabaei Anaraki, R. Dutta Majumdar, N. Wagner, R. Soong, V. Kovacevic, E. J. Reiner, S. P. Bhavsar, X. Ortiz Almirall, D. Lane, M. J. Simpson, H. Heumann, S. Schmidt and A. J. Simpson, Development and Application of a Low-Volume Flow System for Solution-State *in Vivo* NMR, *Anal. Chem.*, 2018, **90**, 7912–7921.

34 G. C. Woods, M. J. Simpson, P. J. Koerner, A. Napoli and A. J. Simpson, HILIC-NMR: Toward the Identification of Individual Molecular Components in Dissolved Organic Matter, *Environ. Sci. Technol.*, 2011, **45**, 3880–3886.

35 J. J. Ellinger, R. A. Chylla, E. L. Ulrich and J. L. Markley, Databases and Software for NMR-Based Metabolomics, *Curr. Metabolomics*.

36 P. Sakhaii and W. Bermel, A different approach to multiplicity-edited heteronuclear single quantum correlation spectroscopy, *J. Magn. Reson.*, 2015, **259**, 82–86.

37 W. Peti, C. Griesinger and W. Bermel, Adiabatic TOCSY for C,C and H,H J-transfer, *J. Biomol. NMR*, 2000, **18**, 199–205.

38 H. Farooq, D. Courtier-Murias, R. Soong, W. Bermel, W. M. Kingery and A. J. Simpson, HR-MAS NMR Spectroscopy: A Practical Guide for Natural Samples, 2013, **17**, 3013–3031.

39 D. E. Koshland and F. H. Westheimer, Mechanism of Alcoholic Fermentation. The Fermentation of Glucose-1-C14, *J. Am. Chem. Soc.*, 1950, **72**, 3383–3388.

40 J. L. Galazzo and J. E. Bailey, Fermentation pathway kinetics and metabolic flux control in suspended and immobilized Saccharomyces cerevisiae, *Enzyme Microb. Technol.*, 1990, **12**, 162–172.

41 M. Ikeda, R. Katsumata and O. Zelder, Hyperproduction of tryptophan by Corynebacterium glutamicum with the modified pentose phosphate pathway, *Appl. Environ. Microbiol.*, 1999, **65**, 2497–502.

42 J. M. Buescher, M. R. Antoniewicz, L. G. Boros, S. C. Burgess, H. Brunengraber, C. B. Clish, R. J. DeBerardinis, O. Feron, C. Frezza, B. Ghesquiere, E. Gottlieb, K. Hiller, R. G. Jones, J. J. Kamphorst, R. G. Kibbey, A. C. Kimmelman, J. W. Locasale, S. Y. Lunt, O. D. K. Maddocks, C. Malloy, C. M. Metallo, E. J. Meuillet, J. Munger, K. Nöh, J. D. Rabinowitz, M. Ralser, U. Sauer, G. Stephanopoulos, J. St-Pierre, D. A. Tennant, C. Wittmann, M. G. Vander Heiden, A. Vazquez, K. Vousden, J. D. Young, N. Zamboni and S.-M. Fendt, A roadmap for interpreting (13)C metabolite labeling patterns from cells, *Curr. Opin. Biotechnol.*, 2015, **34**, 189–201.

43 W. M. De Coen, C. R. Janssen and H. Segner, The Use of Biomarkers in Daphnia magna Toxicity Testing V. In Vivo Alterations in the Carbohydrate Metabolism of Daphnia magna Exposed to Sublethal Concentrations of Mercury and Lindane, *Ecotoxicol. Environ. Saf.*, 2001, **48**, 223–234.

44 W. Wiechert, 13C Metabolic Flux Analysis, *Metab. Eng.*, 2001, **3**, 195–206.

45 A. Marx, A. A. de Graaf, W. Wiechert, L. Eggeling and H. Sahm, Determination of the fluxes in the central metabolism of Corynebacterium glutamicum by nuclear magnetic resonance spectroscopy combined with metabolite balancing, *Biotechnol. Bioeng.*, 1996, **49**, 111–129.

46 C. Zwingmann, N. Chatauret, D. Leibfritz and R. F. Butterworth, Selective increase of brain lactate synthesis in experimental acute liver failure: Results of a [1H-13C] nuclear magnetic resonance study, *Hepatology*, 2003, **37**, 420–428.

47 A. Wacker and D. Martin-Creuzburg, Allocation of essential lipids in Daphnia magna during exposure to poor food quality, *Funct. Ecol.*, 2007, **21**, 738–747.

48 M. Bastawrous, A. Jenne, M. Tabatabaei Anaraki and A. Simpson, In-Vivo NMR Spectroscopy: A Powerful and Complimentary Tool for Understanding Environmental Toxicity, *Metabolites*, 2018, **8**, 35.

49 C. E. Goulden and A. R. Place, Fatty acid synthesis and accumulation rates in daphniids, *J. Exp. Zool.*, 1990, **256**, 168–178.

50 L. Ruess and P. M. Chamberlain, The fat that matters: Soil food web analysis using fatty acids and their carbon stable isotope signature, *Soil Biol. Biochem.*, 2010, **42**, 1898–1910.

51 J. A. G. Duarte, F. Carvalho, M. Pearson, J. D. Horton, J. D. Browning, J. G. Jones and S. C. Burgess, A high-fat diet suppresses de novo lipogenesis and desaturation but not elongation and triglyceride synthesis in mice, *J. Lipid Res.*, 2014, **55**, 2541–53.

52 C. Ettenhuber, T. Radykewicz, W. Kofer, H.-U. Koop, A. Bacher and W. Eisenreich, Metabolic flux analysis in complex isotopolog space. Recycling of glucose in tobacco plants, *Phytochemistry*, 2005, **66**, 323–335.

53 R. Gruetter, E. J. Novotny, S. D. Boulware, G. F. Mason, D. L. Rothman, G. I. Shulman, J. W. Prichard and R. G. Shulman, Localized 13C NMR Spectroscopy in the Human Brain of Amino Acid Labeling from d-[1-13C]Glucose, *J. Neurochem.*, 2002, **63**, 1377–1385.

54 M. D. McCoole, B. T. D'Andrea, K. N. Baer and A. E. Christie, Genomic analyses of gas (nitric oxide and carbon monoxide) and small molecule transmitter (acetylcholine, glutamate and GABA) signaling systems in Daphnia pulex, *Comp. Biochem. Physiol. Part D Genomics Proteomics*, 2012, **7**, 124–160.

55 N. R. Sibson, A. Dhankhar, G. F. Mason, K. L. Behar, D. L. Rothman and R. G. Shulman, In vivo 13 C NMR measurements of cerebral glutamine synthesis as evidence for glutamate-glutamine cycling (hyperammonemianeurotransmitter cycledetoxification), *Neurobiology*, 1997, **94**, 2699–2704.

56 L. Hertz, The Glutamate–Glutamine (GABA) Cycle: Importance of Late Postnatal Development and Potential Reciprocal Interactions between Biosynthesis and Degradation, *Front. Endocrinol. (Lausanne).*, 2013, **4**, 59.

57 A. Bunescu, J. Garric, B. Vollat, E. Canet-Soulas, D. Graveron-Demilly and F. Fauvelle, In vivo proton HR-MAS NMR metabolic profile of the freshwater cladoceran Daphnia magna, *Mol. Biosyst.*, 2009, **6**, 121–125.

58 A. Putman, D. Martin-Creuzburg, B. Panis and L. De Meester, A comparative analysis of the fatty acid composition of sexual and asexual eggs of *Daphnia magna* and its plasticity as a function of food quality, *J. Plankton Res.*, 2015, **37**, 752–763.

View Article Online
DOI: 10.1039/C8FD00213D

59 M. Kariuki, E. Nagato, B. Lankadurai, A. Simpson and M. Simpson, Analysis of Sub-Lethal Toxicity of Perfluorooctane Sulfonate (PFOS) to Daphnia magna Using 1H Nuclear Magnetic Resonance-Based Metabolomics, *Metabolites*, 2017, **7**, 1–13.
60 V. Kovacevic, A. J. Simpson and M. J. Simpson, 1H NMR-based metabolomics of Daphnia magna responses after sub-lethal exposure to triclosan, carbamazepine and ibuprofen, *Comp. Biochem. Physiol. Part D*, 2016, **19**, 199–210.
61 H. L. Wheeler, R. Soong, D. Courtier-Murias, A. Botana, B. Fortier-Mcgill, W. E. Maas, M. Fey, H. Hutchins, S. Krishnamurthy, R. Kumar, M. Monette, H. J. Stronks, M. M. Campbell and A. Simpson, Comprehensive multiphase NMR: a promising technology to study plants in their native state, *Magn. Reson. Chem.*, 2015, **53**, 735–744.
62 B. G. Forde and P. J. Lea, Glutamate in plants: metabolism, regulation, and signalling, *J. Exp. Bot.*, 2007, **58**, 2339–2358.
63 V. R. Young and A. M. Ajami, Glutamate: An Amino Acid of Particular Distinction, *J. Nutr.*, 2000, **130**, 892S–900S.
64 R. A. Harris and E. T. Harper, in *eLS*, John Wiley & Sons, Ltd, Chichester, UK, 2015, pp. 1–8.
65 U. Sonnewald, N. Westergaard, B. Hassel, T. B. Müller, G. Unsgård, F. Fonnum, L. Hertz, A. Schousboe and S. B. Petersen, NMR spectroscopic studies of 13C acetate and 13C glucose metabolism in neocortical astrocytes: evidence for mitochondrial heterogeneity, *Dev. Neurosci.*, 1993, **15**, 351–8.
66 L. Lam, R. Soong, A. Sutrisno, R. De Visser, M. J. Simpson, H. L. Wheeler, M. Campbell, W. E. Maas, M. Fey, A. Gorissen, H. Hutchins, B. Andrew, J. Struppe, S. Krishnamurthy, R. Kumar, M. Monette, H. J. Stronks, A. Hume and A. Simpson, Comprehensive Multiphase NMR Spectroscopy of Intact 13C-Labeled Seeds, *J. Agric. Food Chem.*, 2014, **62**, 107–115.
67 A. P. Deshmukh, A. J. Simpson and P. G. Hatcher, Evidence for cross-linking in tomato cutin using HR-MAS NMR spectroscopy, *Phytochemistry*, 2003, **64**, 1163–1170.
68 R. K. Adosraku, G. T. Choi, V. Constantinou-Kokotos, M. M. Anderson and W. A. Gibbons, NMR lipid profiles of cells, tissues, and body fluids: proton NMR analysis of human erythrocyte lipids, *J. Lipid Res.*, 1994, **35**, 1925–31.
69 M. J. DeNiro and S. Epstein, Mechanism of carbon isotope fractionation associated with lipid synthesis, *Science*, 1977, **197**, 261–3.
70 N. Blair, A. Leu, E. Muñoz, J. Olsen, E. Kwong and D. Des Marais, Carbon isotopic fractionation in heterotrophic microbial metabolism, *Appl. Environ. Microbiol.*, 1985, **50**, 996–1001.
71 T. W.-M. Fan and A. N. Lane, Applications of NMR spectroscopy to systems biochemistry, *Prog. Nucl. Magn. Reson. Spectrosc.*, 2016, **92–93**, 18–53.
72 T. W.-M. Fan and A. N. Lane, Structure-based profiling of metabolites and isotopomers by NMR, *Prog. Nucl. Magn. Reson. Spectrosc.*, 2008, **52**, 69–117.

Figure and Captions

View Article Online
DOI: 10.1039/C8FD00213D

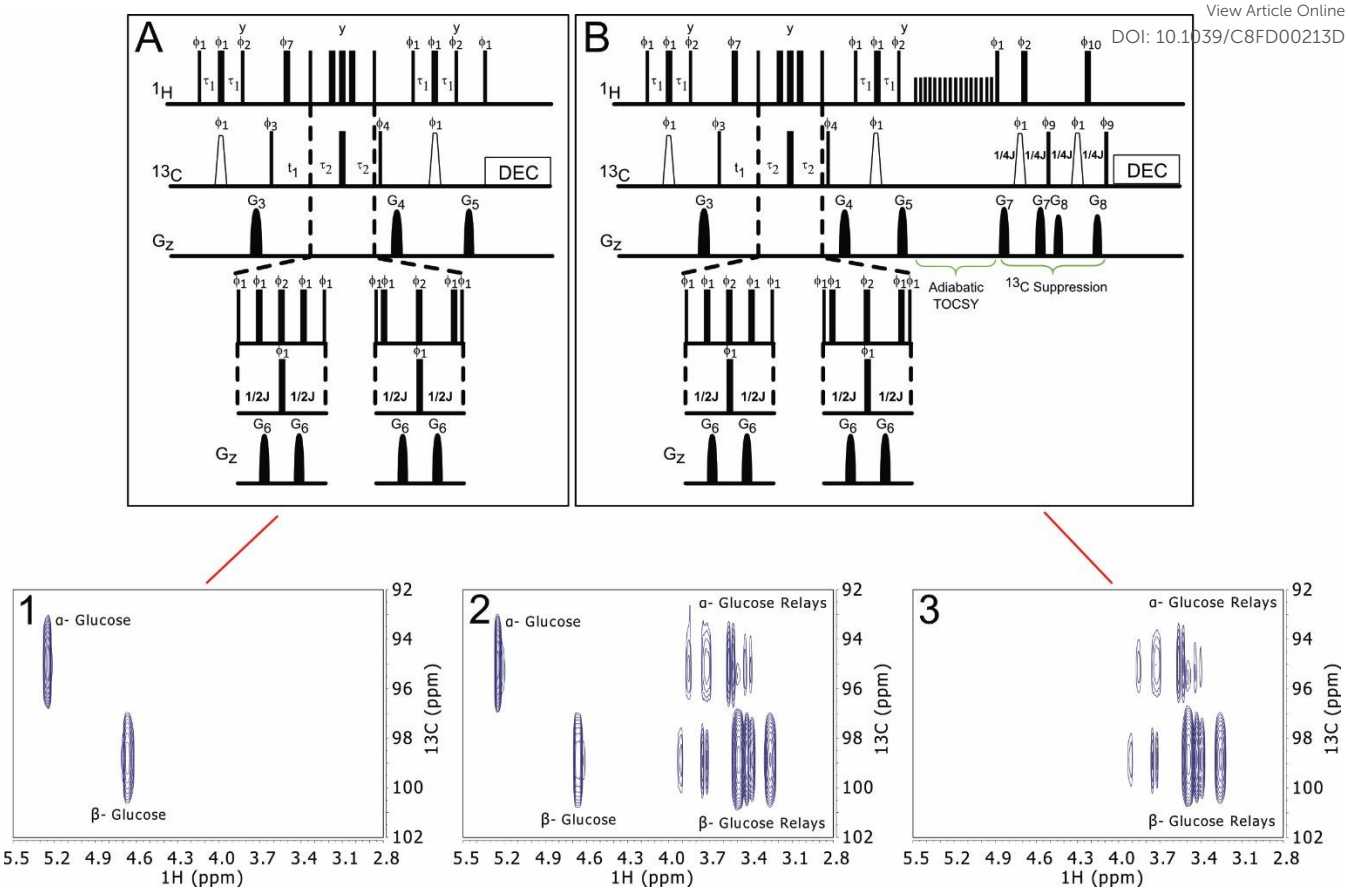

Fig. 1 The basic qualitative sequence. A) A reverse HSQC. Narrow rectangles indicate a 90° pulse, whereas wide rectangles indicate a 180° pulse. Unless otherwise stated, pulses are applied along the x-axis. Open trapezoids represent smoothed chirp pulses for inversion with a pulse length of 500 µs, a sweep width of 60 kHz, defined with 1000 points and with a 20% smoothing of the amplitude on either end. The pulsed field gradients are indicated as filled sine envelopes and are 1ms in length. The amplitudes of the gradient pulses have the following ratio: G3=60%, G4=40%, G5=31%, G6=19%, G7=23%, and G8=13% (with 100% being 53.5 G/cm). The pulsed field gradients are applied along the z-axis followed by a gradient recovery delay of 200 µs. The following phase cycling was used for the pulse sequences: φ_1=0, φ_2=1, φ_3=0 2, φ_4=0 0 0 0 2 2 2 2, φ_7=0 0 0 0 2 2 2 2, φ_8=0 0 2 2, φ_9=0 1 2 3, φ_{10}=1 1 2 2, and φ_{rec}=2 0 2 0 0 2 0 2. B) An adiabatic TOSCY which consists of 16 adiabatic (ca-WURST, 300 µs, 27.3KHz pulses) with the following phase cycle, 0 0 2 2 0 2 2 0 2 2 0 0 2 0 0 2, precedes this sequence, and the additional pulses in panel B are appended. In this part of the sequence the following phase cycling was used: φ_1=0, φ_2=1, φ_9=0 1 2 3, φ_{10}=1 1 2 2, and φ_{rec}=0 2 2 0 2 0 0 2. The bottom panel shows the results of these sequences on 1-^{13}C-Glucose. Sequence A leads to panel 1 in which only the one bond ^{1}H-^{13}C bonds are detected. Panel 2 shows the result of data collected after the TOCSY block in B. At this point the data resemble and HSQC-TOCSY (note this data is not actually collected but is included for clarity). Panel 3 shows the result of sequence B. In this case, the ^{1}H-^{13}C bonds are subtracted. Leaving only signal from ^{1}H-^{12}C that is in the same spin system as a ^{13}C. In practice the data collection is interleaved with sequence A being collected for first slice and then sequence B being collected for the second slice and so on. The data are then split at the end of the experiment to give panels 1 and panels 3.

View Article Online
DOI: 10.1039/C8FD00213D

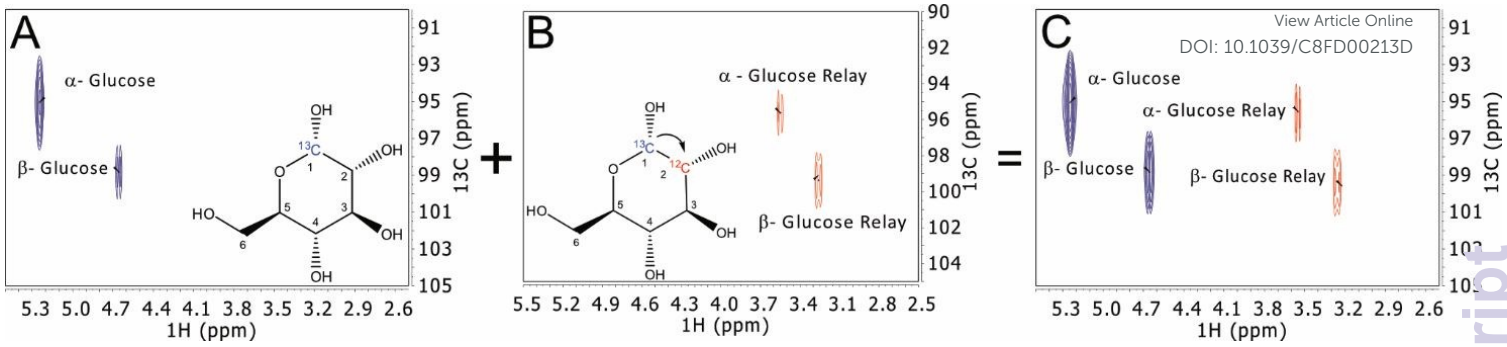

Fig. 2 Examining the process of monitoring ^{13}C-^{12}C Bonds using 1-^{13}C-Glucose. A) 2D reverse HSQC that only detects ^{13}C atoms (i.e. result from sequence 1A), the glucose molecule contains the labelled carbons in blue. B) 2D ^{13}C-^{12}C sequence with a 30ms TOCSY mixing time that selectively detects COSY-like relays and subtracts the signals from ^{13}C (i.e. the result from sequence 1B). C) The overlaid spectra of the 2A and 2B. ^{13}C are show in blue while relays to ^{12}C are shown in red. With a 30ms TOCSY mixing if a blue crosspeak is seen on the same row as the red crosspeak it means they are directly bonded in the molecule.

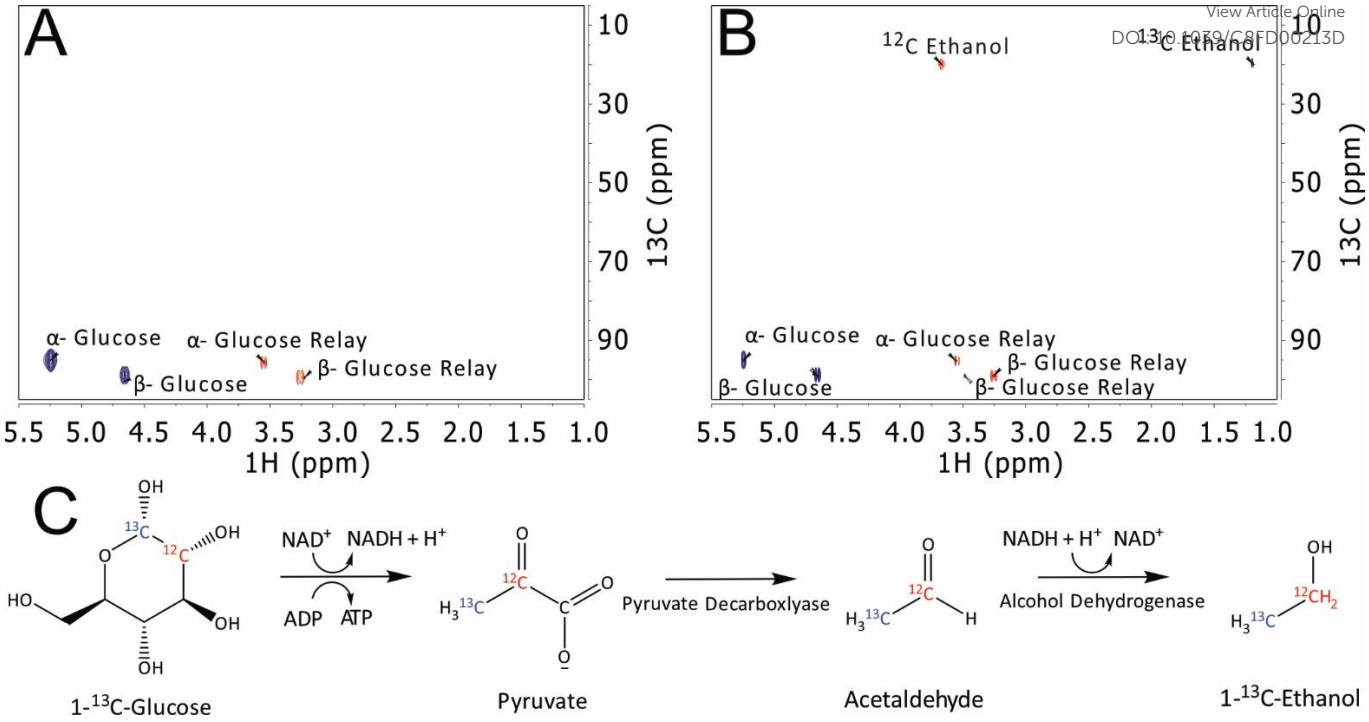

Fig. 3 Following a simple process of fermentation. 1-^{13}C-Glucose was mixed with Baker's yeast (*Saccharomyces cerevisiae*) for 24 hours inside the NMR to monitor the formation of 1-^{13}C-ethanol. Carbons 1 and 2 in glucose are used to form ethanol through fermentation, A) The same overlaid spectrum from Figure 2C prior to the fermentation reaction, B) 24 hours after the addition of yeast. ^{13}C is seen in blue, and the ^{12}C relays are in red. In this case, ethanol is formed with methylene group from ^{12}C and the methyl group from ^{13}C. C) Simplified fermentation process with 1-^{13}C-glucose.

View Article Online
DOI: 10.1039/C8FD00213D

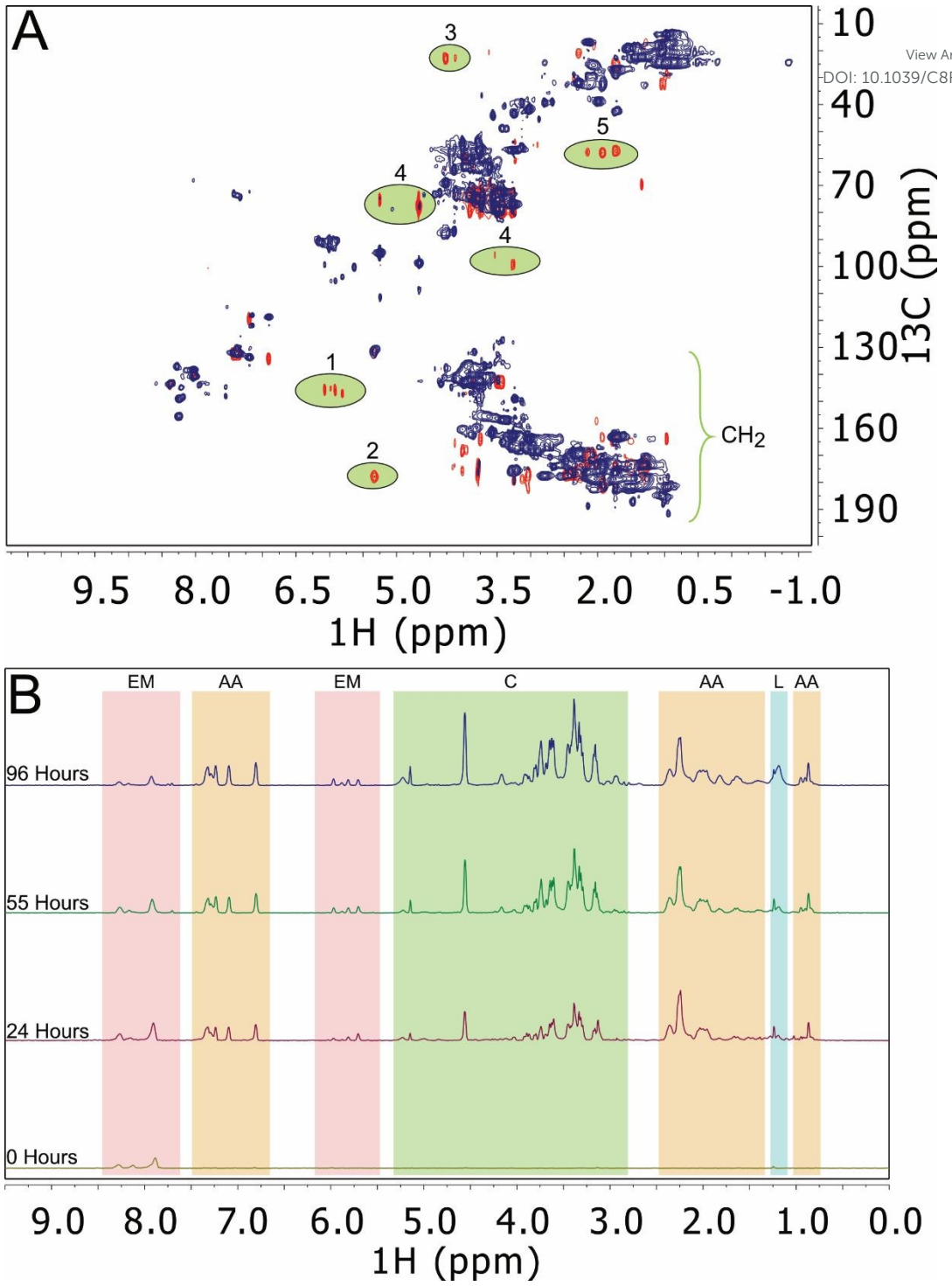

Fig. 4 Sequence applied to *Daphnia magna* extracts. Organisms were enriched for two weeks from birth with 99% ^{13}C enriched algae. They were then switched to natural abundance ^{12}C algae and monitored for four days. Samples were taken every 24 hours and extracted using a phosphate buffer. A) Overlaid 2D NMR of the 96-hour sample. Blue is the ^{13}C remaining in the organisms and red is the ^{12}C relays to the new bonds formed. There are five regions of interest highlighted in green. 1) Adenine from ^{13}C bonding with ^{12}C ribose from the algae used in energy formation, 2) ^{13}C lipids containing ^{12}C unsaturation indicative of lipid synthesis, 3) Protons in the ^{13}C lipid chains relaying to ^{12}C adjacent to oxygen, 4) Carbohydrate components including a mix of carbon enrichment in glucose as it moves through the TCA cycle and glycogenesis, 5) A mixture of glutamate and glutamine amino acids. B) 1D ^{1}H projections for all the time points showing the uptake and use of ^{12}C in the Daphnia. EM = Energy Molecules, AA = Amino Acids, C = Carbohydrates, and L = Lipids.

View Article Online
DOI: 10.1039/C8FD00213D

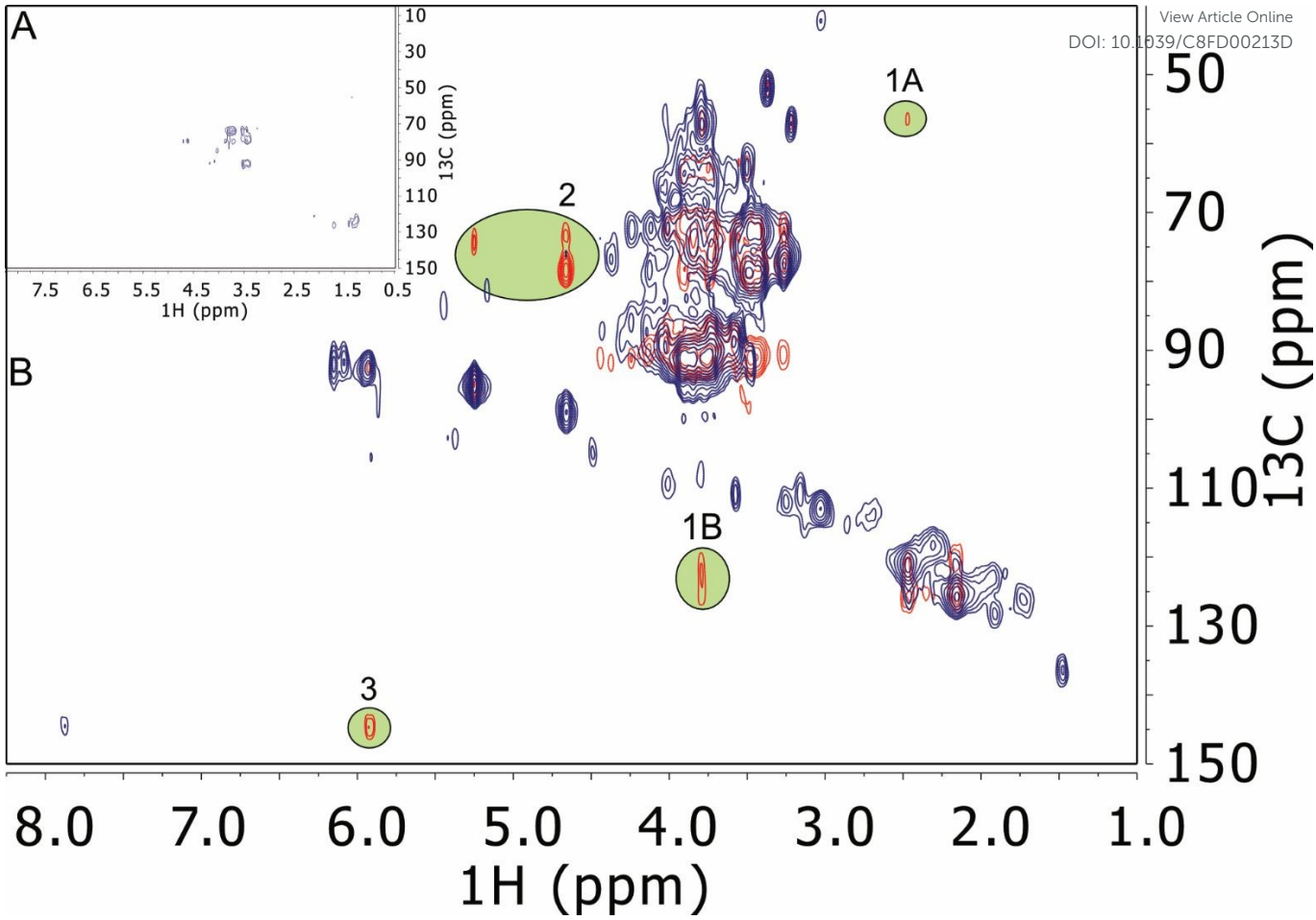

Fig. 5 *Arabidopsis thaliana* grown in the dark with $^{13}C_6$-Glucose as the primary carbon source. A) One day of growth with ^{13}C in blue and an absence of relays due to the lack of new bond formation. B) Seven-day growth of plants with ^{13}C in blue and ^{12}C relays in red. Three areas of interest are highlighted in green. 1A) $\alpha^{13}C$-$\beta^{12}C$ glutamate relays, 1B) $\alpha^{12}C$-$\beta^{13}C$ glutamate relays, an essential amino acid in plants, 2) Relays from glucose from glycolysis and TCA cycle, 3) Formation of energy molecules derived from the glucose and TCA cycle.

View Article Online
DOI: 10.1039/C8FD00213D

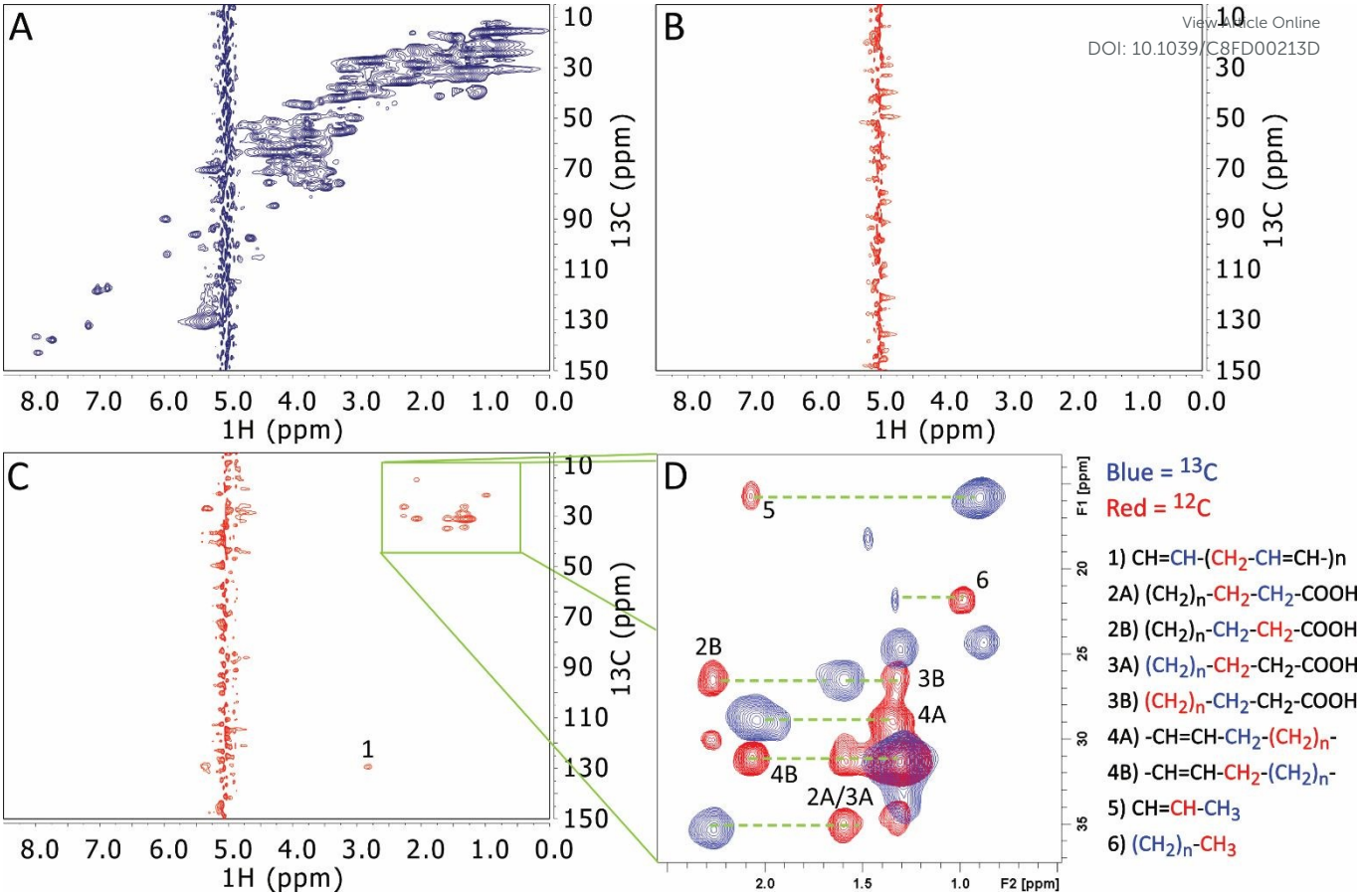

Fig. 6 Testing the ^{13}C-^{12}C sequence on an *in-vivo* sample of *Daphnia magna*. In this case, the *Daphnia* were cultured from birth for two weeks using 99% enriched ^{13}C algae, and then switched to natural abundance ^{12}C algae for 9 days. A) 2D HSQC of day zero *Daphnia* (i.e. not ^{12}C fed), B) ^{13}C-^{12}C spectrum at day zero, no relays were detected due to the lack of ^{12}C in the system (note the streak at 5 ppm is residual water), C) ^{13}C-^{12}C relays of D*aphnia* after nine days of exposure to ^{12}C algae as the food source. Relays have started to appear due to the assimilation of the new food into their biomass, D) An expansion of the lipid region highlighting the new bonds that are formed.

View Article Online
DOI: 10.1039/C8FD00213D

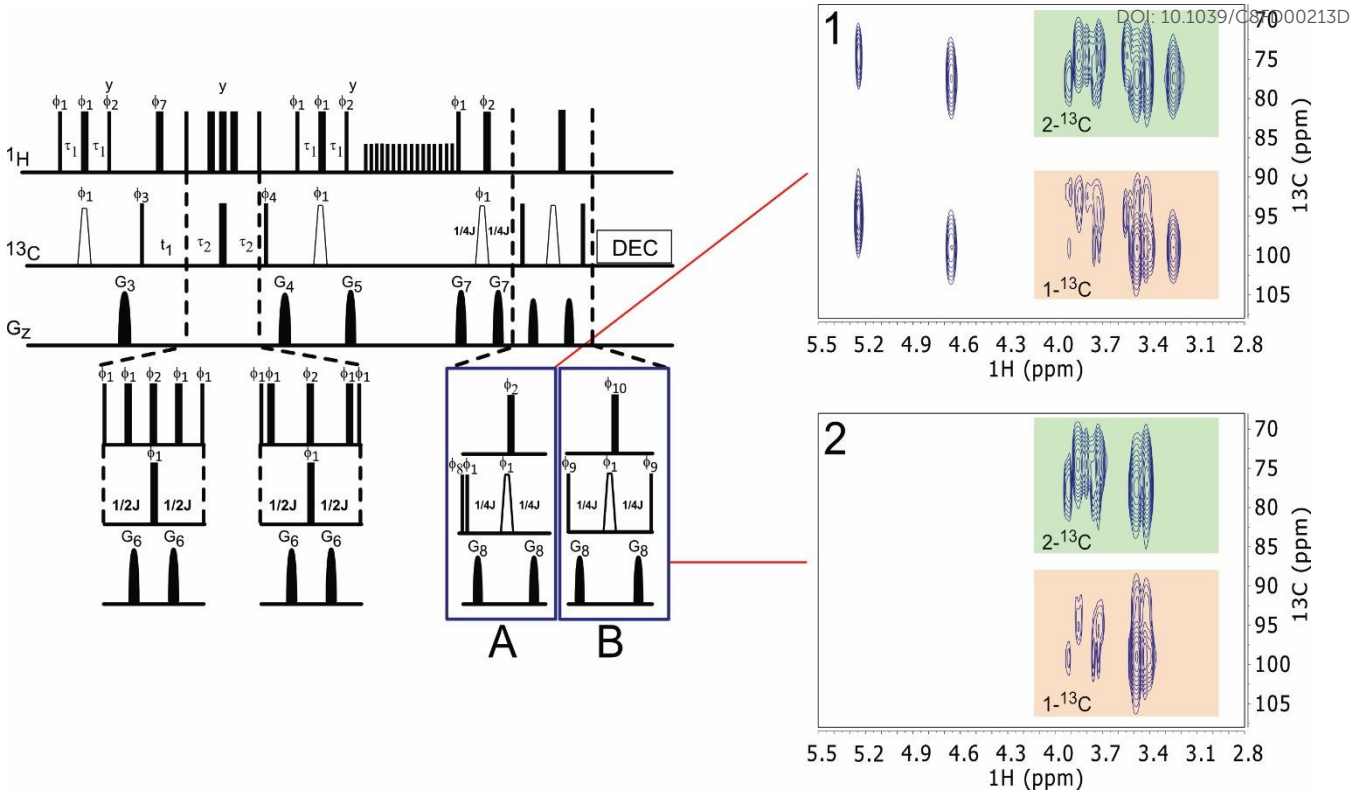

Fig. 7 The basic quantitative sequence. Block B produces the same result as Figure 1B in that the ^{13}C signals are subtracted to leave only relays to ^{1}H-^{12}C. Figure 7A is derived from 7B with goal to keep the pulses, durations and timing identical between the two sequences. By reorganizing the x-filter element (block B) to become a spin-echo on carbon, and eliminating the carbon phase cycling (i.e. φ8= 0 in block A), block A essentially does nothing and allows signals from both ^{1}H-^{12}C and ^{1}H-^{13}C to pass. The data from A and B are collected in an interleaved fashion. Narrow rectangles indicate a 90° pulse whereas wide rectangles indicate a 180° pulse. Unless otherwise stated, pulses are applied along the x-axis. Open trapezoids represent smoothed chirp pulses for inversion with a pulse length of 500 µs, a sweep width of 60 kHz, defined by 1000 points and with a 20% smoothing of the amplitude on either end. The pulsed field gradients are indicated as filled sine enveloped and are 1ms in length. The amplitudes of the gradient pulses have the following ratio: G3=60%, G4=40%, G5=31%, G6=19%, G7=23%, and G8=13% (with 100% being 53.5 G/cm). The pulsed field gradients are applied along the z-axis followed by a gradient recovery delay of 200 µs. The following phase cycling was used for the pulse sequences: φ_1=0, φ_2=1, φ_3=0 2, φ_4=0 0 0 0 2 2 2 2, φ_7=0 0 0 0 2 2 2 2, φ_8=0, φ_9=0 1 2 3, φ_{10}=1, and φ_{rec}=0 2 0 2 2 0 2 0. The adiabatic TOCSY is comprised of 16 adiabatic (ca-WURST, 300 µs, 27.3KHz pulses) with the following phase cycle, 0 0 2 2 0 2 2 0 2 2 0 0 2 0 0 2. Sequence 7A results in spectra one, where both the ^{13}C and ^{12}C is acquired. In this case, 1,2-^{13}C-Glucose was used, 7B subtracts the ^{13}C information leaving only the ^{12}C as can be seen in spectra two. This allows for quantification by examining signal loss between 7A (the control) and 7B (the ^{12}C-only spectrum), the difference being the % ^{13}C at a specific site.

View Article Online
DOI: 10.1039/C8FD00213D

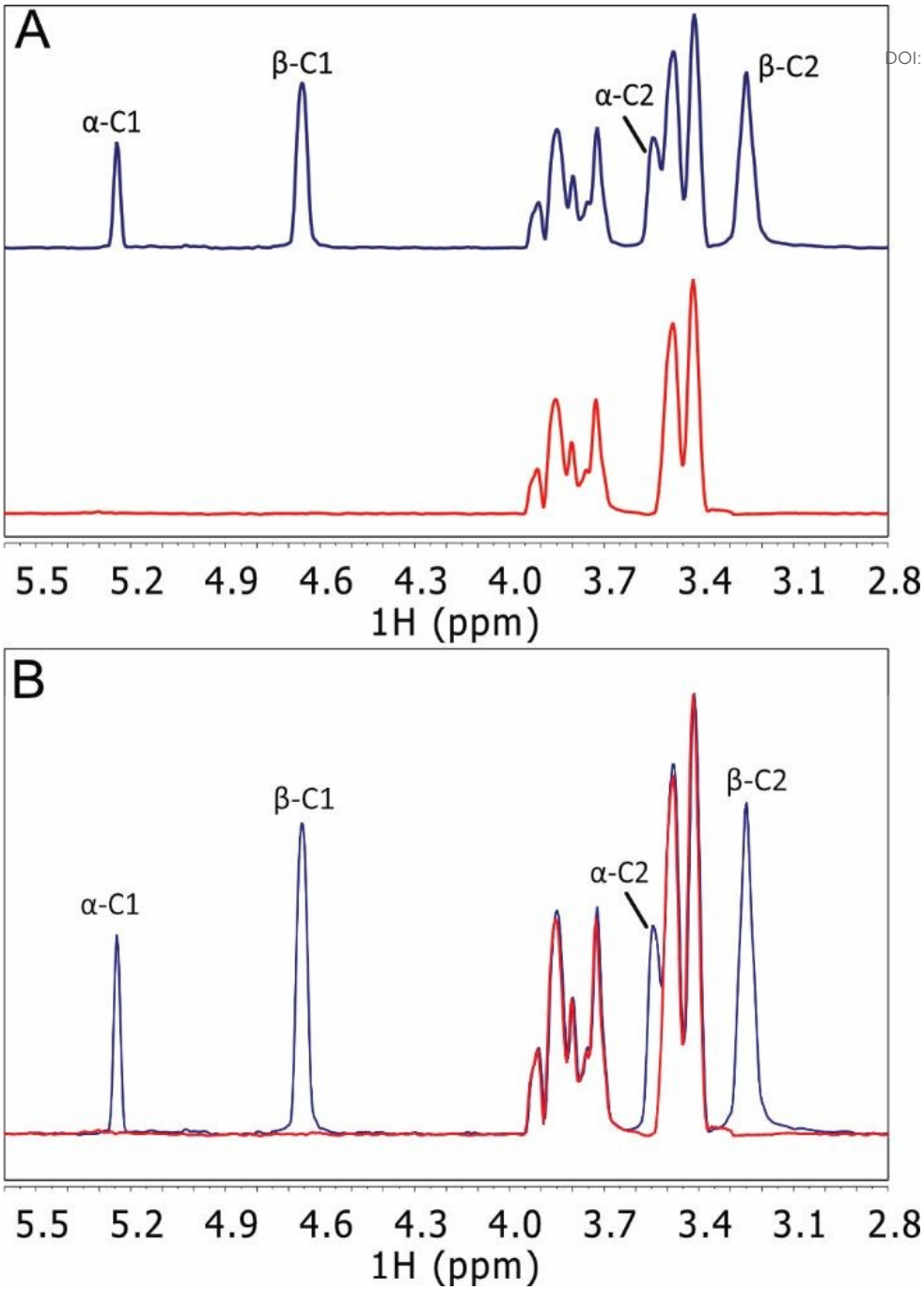

Fig. 8 A simple example of the potential for quantification on 1,2-^{13}C-Glucose. A) Top spectra is the ^{1}H projection from the quantitative reference (both protons on ^{12}C and ^{13}C appear), and the bottom is the ^{12}C-only sequence (only ^{1}H on ^{12}C are observed), B) The superimposed spectra shows the ^{13}C completely cancel resulting in the red ^{12}C signals. This theoretically allows for quantification by measuring the signals loss in the ^{12}C-only sequence relative to the reference which represents the % ^{13}C at that specific position within the molecule.